Heritage At-Risk:

Vulnerability of Cultural Resources along Florida's Coast to Sea Level Rise and Hurricanes

ALEX ZARLEY
SHELLEY WITTE
GENEVIEVE BURGESS

University of Wisconsin-Madison Geography

TABLE OF CONTENTS

Objectives

Rising sea levels and modern development pose a threat to the 102 archaeological sites in the National Register of Historic Places located within 5km of Florida's coast. With 10% of its landmass less than 1m above mean sea-level (Noss 2011, 4) and over 2,100km of coastline (FOCC 2010, 1), Florida's coastal cultural resources are especially vulnerable to increased sea-level rise over the next century (Thieler and Hammar-Klose 2000; Thieler and Hammar-Klose 1999). Excavation and documentation of all coastal sites is impossible. However, cultural resource managers can use vulnerability indices to prioritize preservation and documentation of resources most at-risk before they are lost forever. Therefore, we will be creating a cultural resource vulnerability index (CRVI) for Florida's coastal archaeological sites based on their location, shoreline vulnerability (SV), and land use. This will allow us to map and rank the vulnerability of Florida's coastal archaeological sites.

Our main project goal is to rank the vulnerability of the archaeological sites in our study area in order to produce a decision-making tool for cultural resource managers in Florida. This will produce a map and infographics showing vulnerability scores and rankings. We also want to explore the impact of events, such as hurricanes, on the erosion rates of Florida. Finally, we hope to determine what, if any, impact hurricanes have on the shoreline vulnerability of Florida's coast in order to determine if hurricane's and other climate related events should be taken into account in future coastal vulnerability and cultural resource vulnerability indices.

Background and Site Setting

Twenty-first century sea-level rise poses a risk to cultural resources in coastal regions. Ancient settlements, architectural features, artifacts and burials along the coast are frequently inundated, exposed and washed away by the deleterious effects of wind and water. (Reeder-Myers 2015, 436-437; Robinson et al. 2010, 312-313). The fill around these archaeological sites holds information that is key to understanding past societies, and as soon as the fill is disturbed, that knowledge is lost (Reeder-Myers 2015, 437; Van Rensselaer 2014, 373, 379; Reeder et al. 2010, 187). This makes identifying and documenting those sites most at-risk of critical importance (Robinson et al. 2010, 313).

Because of the pace at which archaeological sites are being lost to climate change, researchers have begun to model vulnerability of and risk to archaeological sites in coastal

regions in hopes of identifying coastlines on a national and regional scale (Revell et al. 2011; Thieler and Hammar-Klose 2000; Thieler and Hammar-Klose 1999), and specific archaeological sites on a local scale (Reeder-Myers 2015; Van Rensselaer 2014; Reeder et al. 2012; Westley et al. 2011; Robinson et al. 2010; Fitzpatrick et al. 2006), that are particularly vulnerable to the effects of climate change and rising sea levels. The dynamic and uncertain nature of the effects of climate change make the importance of identifying vulnerable areas as soon as possible even more important.

Florida is especially vulnerable to the effects of sea-level rise. The USGS National Assessment of Coastal Vulnerability to Sea-Level Rise for the contiguous United states showed Florida's entire Atlantic coast having a moderate to very high vulnerability (Thieler and Hammar-Klose 1999), and its Gulf coast having a mostly moderate risk (Thieler and Hammar-Klose 2000). Florida also has more than 2,000km of coastline, the maximum elevation of the entire state is less than 122m (FOCC 2010, 1), and approximately 10% of the state sits one meter or less above sea-level (Noss 2011, 4). The most recent IPCC report predicts a rise of 26 - 82cm of mean sea-level globally by 2100 (IPCC 2014, 59-60). Other estimates believe the rate of sea-level rise (SLR) will increase as we move through the 21st century and predict up to 200cm of rise (Van Rensselaer 2014; Saha et al. 2011, 82; Reeder et al. 2010, 190; Erlandson 2008, 167). A 30cm rise in sea level causes coastal systems to become erosional (Saha et al. 2011, 82), making even the most conservative estimates of sea-level rise potentially catastrophic to Florida's coastal areas. A rise in relative sea level of 30cm in Florida will cause the rapid retreat of shorelines with sand beaches, mangrove swamps, salt marshes, and marl levees (Wanless et al. 1994, 200). Nearly all of Florida's coast fits into one of these categories (Thieler and Hammar-Klose 2000; Thieler and Hammar-Klose 1999). A 30cm rise in sea level will also lead to inundation of low-lying coastal areas and a loss of freshwater resources due to saline intrusion in ground water (Wanless et al. 1994, 200). In addition, Florida is more likely to be struck by a hurricane than any other state, with a hurricane making landfall every two years and a strong hurricane hitting the state every four years (Malmstadt et al. 2009, 108). The loss of cultural resources to hurricanes can be catastrophic, with an estimated 1000 historical and archaeological sites along the northern coast of the Gulf of Mexico having been destroyed by Hurricane Katrina alone (Erlandson 2008, 168). Therefore, Florida's coastal archaeological sites are at risk of disappearing if action is not taken to document, excavate, or preserve them.

Methodology

We will be assessing the vulnerability of coastal archaeological sites listed in the National Register of Historic Places in Florida by constructing a cultural resource vulnerability index (Reeder-Myers 2015; Reeder et al. 2012). Using geographic information systems to quantify the risk of individual archaeological sites by creating CRVI's allows researchers and cultural resource managers to make informed decisions based on the effects of erosion, SLR and other coastal hazards (Van Rensselaer 2014, 374). All the vulnerability indices discussed in this paper have relied either on historical data (Reeder-Myers 2015; Thieler and Hammar-Klose 2000), or modeling future sea-level rise (Westley et al. 2011). We will be using historical data to create our vulnerability indices because the data for this methodology is more robust. The vulnerability of each site is assessed by its location in the landscape, how vulnerable the closest shoreline to the site is, and the modern land use at and around the site (Reeder-Myers 2015, 437). A score is then generated for each site using the following equation (Reeder-Myers 2015, 437):

$$\mathrm{CRV} = \frac{2(\mathrm{D} + \mathrm{E}) + 3(\mathrm{SV}) + 2(\mathrm{LU})}{3}$$

This equation places the greatest emphasis on the site's distance from the coast (D) and its elevation (E), followed by the vulnerability of the shoreline closest to the site (SV) and the modern land use near the site (LU). Raw values are normalized on a 1 to 5 scale for distance, elevation and shoreline vulnerability (Reeder-Myers, personal communication). Land use is ranked categorically on a 1 to 5 scale (Reeder-Myers 2015, 438-439). Each of these key concepts is discussed in detail below (Figures 1 and 2).

Shoreline vulnerability indices help researchers quantify coastal hazards using a general equation (Van Rensselaer 2014, 376). We used geomorphology(a), coastal slope(b), relative sea-level rise(c), shoreline erosion(d), wave height(e), and tidal range(f) to calculate SV. The USGS performed a study of the entire coastline of the contiguous United States and calculated SV with an unweighted formula (Thieler and Hammar-Klose 2000, 1999):

$$\mathrm{SV} = \sqrt{\frac{\mathrm{a} * \mathrm{b} * \mathrm{c} * \mathrm{d} * \mathrm{e} * \mathrm{f}}{6}}$$

The issue with unweighted formulas is that they assume all factors are of equal importance. The scope of this project did not include investigation into the importance of variables to determine if

an unweighted formula, such as this one, would be most appropriate or if a weighted formula could provide more accurate results.

Reeder-Myers performed a study on a regional scale of sites in California, Texas and Virginia and calculated SV with a weighted formula (Reeder-Myers 2015, 439):

$$SV = \frac{4(a + b + c) + 3(d) + 2(e + f)}{6}$$

We did not use Reeder-Myers' formula, however, since we were unable to obtain justification for the weights in the formula. Again, an attempt to validate the weights in this formula was outside the scope of this project. With more time and resources, it would have been appropriate to investigate the potential of a weighted shoreline vulnerability formula specific to Florida**.** In addition, we explored the effects of hurricanes on the vulnerability of coastlines and have that as its own variable outside of the SVI. By overlaying historic hurricane tracks in the coastal areas for which we have historic shoreline change data, we attempted to quantify the impact of hurricanes on shoreline change.

Due to concerns of looting, the Florida State Archaeologist's office could not provide any data as to the location of specific archaeological sites. However, they did provide a polygon shapefile with all 1718 sites in Florida on the National Register of Historic Places. Other CRV studies used a 5km coastal buffer as their study areas (Reeder-Myers 2015, 437), so we performed a 5km buffer inland from the coast. We first attempted to define the coast as the 0m elevation contour line derived from NOAA LiDAR data (Digital Coast). That did not produce an accurate coastal representation since many areas of Florida have a coastal elevation below 0m. Another possibility would have been to manually digitize a shoreline using the LiDAR datasets available, but time and resources did not allow for that. For the sake of expediency, the shoreline data we used was a vector from NOAA ENC created with a resolution of 1:150,001 – 1:600,000 (NOAA Office of Coastal Survey). The 5km buffer from this coastline gave us 1105 sites. We then reviewed the remaining sites and manually removed sites that were not archaeological sites, parks or excavations, which left us with 102 sites. A further review of the data to remove shipwrecks and other sites already underwater left us with 67 sites to rank with our CRVI.

The key concept location consists of elevation and distance (Figure 1). Elevation is defined as meters above mean sea level (Reeder-Myers 2015, 439-440; Reeder et al. 2012, 193). The digital elevation model (DEM) used to calculate site elevation was a 5m gridded composite

with a 1cm vertical resolution created by the University of Florida GeoPlan Center (see Table of Data Sources) using LiDAR data from NOAA coastal LiDAR, Florida Fish and Wildlife Conservation Commission and Northwest Florida Water Management District. LiDAR data was collected from 2004-2010. Contours of 1 and 2m, as well as 5 and 10ft, were used throughout the state, so vertical accuracy varies, but all data are within National Map Accuracy Standards for vertical accuracy, which require 90 percent of all points tested to be within ½ of the contour interval. Reeder-Myers used the polygon centroid of sites to calculate elevation (2015, 440). Since the vertical resolution of our DEM is 1cm, as opposed to the approximately 10m resolution used by Reeder-Myers' (Reeder-Myers 2015, 440), we calculated the site elevation by averaging all elevation values within the site polygon. For cells split by polygon arcs, we counted the cell as part of a site if more than 50% of the area of the cell was in the site.

After mean elevations were calculated for each site, we normalized the values on a 1 to 5 scale, with 1 representing the highest elevations (Table 3). The relationship between elevation and coastal vulnerability is not linear (Reeder-Myers 2015, 439), with a site sitting 1m above sea level being exponentially more vulnerable to sea level rise than a site 5m above sea level. In addition, the distribution of the raw elevation values was skewed heavily to the right. Therefore, we used a geometric classification scheme in ArcGIS that is meant to highlight differences within a cluster (New Mexico's Indicator-Based Information System, "Data Grouping Options for NM-IBIS Maps"), which we had with our elevation values.

Distance is defined as the shortest straight-line distance in meters from a site to the coastline (Figure 1). As with elevation, previous studies used the polygon centroid of sites to measure distance (Reeder-Myers 2015, 439-440; Reeder et al. 2012, 192-193). We measured the shortest planar distance from the edges of each site polygon because our data has a higher horizontal resolution than previous CRVI studies. We normalized distance values on a 1 to 5 scale, with 1 representing the farthest site distance from the coast. As with elevation, distance does not have a linear relationship with risk (Reeder-Myers 2015, 439) and the distance distribution was skewed right. We again used a geometric classification scheme to highlight differences within a cluster with a right-skewed distribution (NM-IBIS, "Data Grouping Options for NM-IBIS Maps").

The key concept of shoreline vulnerability (SV) is calculated based on geomorphology, coastal slope, relative sea-level change, shoreline erosion, tidal range, and wave height (Figure

1). We used a planar distance to identify the nearest point on the coastline to each site's polygon edge, and used those points on the shore to calculate values for each variable in the SVI. We will refer to these points as coastal SV points throughout this paper.

Geomorphology is defined as the erodibility of the underlying sediments and is one of the major contributors to the vulnerability of shorelines (Thieler and Hammar-Klose 2000). Geomorphology categorical values were derived from aerial photography and satellite imagery in the USGS CVI study (Thieler and Hammar-Klose 2000; Thieler and Hammar-Klose 1999). We did not have the time or resources to reevaluate shoreline geomorphology with updated images, so we extracted values from the USGS CVI study that intersected our coastal SV points. The Florida coastline only contains geomorphology that falls into the three highest categories for vulnerability: (3) low cliffs and alluvial plains; (4) cobble beaches, estuaries and lagoons; and (5) barrier/sand beaches, marshes, and mud flats (Figure 3). Since we did not have the original landform types associated with the category values (Table 4), we did not use separate classifications for our two site vulnerability calculations. Therefore, the geomorphology variable did not have a great influence on the variability between the two ranking systems we used for site vulnerability.

Coastal slope measures the relative risk of a stretch of coastline to inundation, as well as its potential for shoreline retreat. Low-sloping areas will experience more rapid shoreline retreat and be more susceptible to inundation from sea-level rise, as well as storm surges (Thieler and Hammar-Klose 2000; Thieler and Hammar-Klose 1999). To compute coastal slope, the USGS study and Reeder-Myers' study used topographic and bathymetric elevation data that extended 50km seaward and landward from the coast. They then used a 10km radius for each coastal cell to identify the highest and lowest elevations and calculated the slope percentage for each cell, adjusting the radius where necessary if the 10km extended over the continental shelf (Reeder-Myers 2015, 440; Thieler and Hammar-Klose 2000; Thieler and Hammar-Klose 1999). The topobathic/bathymetric NOAA LiDAR is incomplete for Florida, and several data sources reclassified water cells to all be -1. Therefore, we used NOAA bathymetric data with 90m horizontal resolution and 1m vertical resolution for our seaward measurements. We used the 5m gridded DEM with 1cm vertical resolution for our landward elevation values (see table of data sources). Since our study area extended only 5km landward, we used a 5km radius when identifying the maximum and minimum elevation values for each coastal SV point. Coastal slope

was recorded as a percentage by dividing the elevation change by the distance between the two extreme points and then multiplying by 100. Several points within the 5km buffer had the same maximum or minimum values. To determine which points to use in our slope measurement, we calculated the planar distance between each maximum elevation point and all other minimum elevation points within each buffer and vice versa. We then took the pair of extreme elevation points for each buffer that had the shortest planar distance between them. By using the shortest distance between the maximum elevation points, we calculated the steepest possible coastal slope percentage for each coastal SV point.

Because of lack of available high-resolution bathymetric data for the entire Florida coast, we used two separate spatial and vertical resolution datasets. This should not introduce much error into the final results for two reasons. The shoreline serves as a natural barrier between the two datasets, which means that the maximum elevation always came from one dataset, while the minimum always came from the other. In addition, we were only using one point from each dataset to calculate coastal slope. Therefore, any error that might have been introduced when calculating this variable would be minimal.

After slope percentages were calculated for each coastal SV site, we normalized the values on a 1 to 5 scale using the Jenks method in ArcGIS, with 1 representing the steepest slopes (Thieler and Hammar-Klose 1999). We wanted to set our class breaks where the biggest differences in the values were, so the Jenks method was appropriate (de Smith et al. 2015, "Classification and Clustering").

Relative sea level change is the increase or decrease in mean water elevation over time. The rate of change in sea level is measured in millimeters per year and is calculated from historical monthly sea level data collected by National Ocean Service (NOS) tide gauge stations along the Florida coast. (Reeder-Myers 2015, 440; Thieler and Hammar-Klose 2000; Thieler and Hammar-Klose 1999). For this original layer, data was collected from the Center for Operational Oceanographic Products and Services' (CO-OPS) Sea Level Trends map. CO-OPS computed the sea level trends for Florida's 15 tide gauge stations using, at minimum, 30 years of observations. Measurements were averaged by month, with the effects of episodic events, such as hurricanes, removed. Since the trends are computed locally, they take into account global volumetric changes of ocean water (i.e. added water from glaciers, expansion due to warming, and changes in ocean basin shape), as well as local tectonic processes (i.e. uplift or subsidence) (NOAA,

2016; Thieler and Hammar-Klose 2000). Along with the trend data, we collected the geographic locations of the tide gauge stations in order to create a shapefile of the data. We used the spline method to interpolate the trend values along the coast of Florida as a 45m raster. We chose spline to produce a surface that went through the 15 data points and selected the tension option in order to make that surface conform more closely to the data points. Setting the weight parameter (φ) to 10 produced the smoothest surface with a range of values that were close to the range of values for the data (Esri, 2016a; Esri, 2016b). The raster values were then reclassified into 5 categories based on natural breaks for the Florida classification and the breakpoints from the USGS CVI study for the other (Table 4). A score of 1 was assigned to cells with the smallest sea level rise values.

Historical shoreline erosion or accretion was measured in meters per year (Reeder-Myers 2015, 440; Thieler and Hammar-Klose 2000; Thieler and Hammar-Klose 1999). This rate was calculated by the USGS Center for Coastal and Watershed Studies (Morton and Miller 2005; Morton et al. 2004). They used maps, NOAA Topographic Sheets, aerial photography, and LiDAR to extract shoreline data for four periods: mid-late 1800s, 1920s-1940s, 1960s-1980s, and 1999. Rates were then calculated using least squares linear regression over these four historic shorelines at 50m coastal transects, which are lines perpendicular to the coast (Morton and Miller 2005, 3-5). These rates were stored in a vector shapefile and covered approximately 50% of Florida's coastline (Map 6). Because of the high density and number of points, we used the kriging method for interpolation. After reviewing the semivariogram, we decided that ordinary kriging with a Gaussian semivariogram was appropriate. The interpolated raster did not cover 5 coastal SV points located in the Florida Keys, so we extracted the raw historical erosion rate from the USGS CVI shoreline vector file where it intersected those five points.

We recorded rates of shoreline erosion with negative values and shoreline accretion with positive ones. These values were then normalized on a 1 to 5 scale, with 1 representing the highest accretion rates (Thieler and Hammar-Klose 1999), using the Jenks method to classify the data where the largest distances between data existed (de Smith et al. 2015, "Classification and Clustering").

Tidal range is the vertical difference between the mean high water and mean low water elevations for a given site and is measured in meters (Thieler and Hammar-Klose 1999). Data for the mean tidal range was retrieved using the CO-OPS Sensor Observational Service's spatial-

temporal query website (NOAA, 2016). We selected all tide gauge stations along Florida's coast from the current epoch and the query returned a CSV file containing each station's geographical location as well as its mean high water level and mean low water level. A new field, the mean tidal range, was populated from differencing the mean high water level and mean low water level for each station. This data file was then converted into a point shapefile as one of our original data layers. The mean tidal range point values were interpolated along the entire coast using ordinary kriging. Again, this geostatistical method is used when there is a significant number of data points (in this case, 595 tidal stations), and also when there there is no known overall trend in the data. The mean tidal range was then reclassified into five categories using natural breaks for one reclassification and the breakpoints from the USGS CVI study (Table 4) for the other.

Shoreline vulnerability researchers have classified tidal ranges in different ways. In one study, high-tide ranges were assigned a high vulnerability score due to association with stronger tidal currents and their ability to erode sediment along the coast (Gornitz 1997, 27). However, more recent studies have instead given higher vulnerability scores to coastlines with low-tide ranges (Reeder-Meyers 2015; Thieler and Hammar-Klose 1999), asserting that storms have a greater potential to damage a micro tidal coastline since those coastlines are essentially always near high tide and are thus more susceptible to inundation from storm surges (Thieler and Hammar-Klose 1999). Keeping in line with the latter two studies we based our project on, we gave the lowest vulnerability score to the largest mean tidal range. In our analysis, we looked at the geographic correlation of the tidal range and erosion by differencing the final raster layers and there was no clear geographic patterning showing that high erosion rates were connected with either high or low tidal ranges. We then created a Pearson's correlation matrix to explore the connection between erosion and mean tidal range (Table 5). The matrix revealed a slight positive correlation (with a significant p-value) between erosion and mean tidal range with a Pearson's $r = 0.35$.

Mean wave height is the distance in meters between the wave trough and wave crest and was calculated as a yearly average. Wave height measures the energy of waves and their ability to move beach sand and other coastal materials. We used mean wave height as recorded at NOAA buoys along the coast of Florida to represent this variable (Reeder-Myers 2015, 440; Thieler and Hammar-Klose 1999). After examining the semivariogram, we determined ordinary linear kriging was the most appropriate interpolation method. We extracted mean wave height

values from the interpolated layer at each of the coastal SV points. These values were again normalized on a 1 to 5 scale, with 1 representing the lowest mean wave heights, using the Jenks method.

Land use quantifies the vulnerability of archaeological sites to modern land use (Reeder-Myers 2015, 440). We used the 10m land cover raster data from the Florida Fish and Wildlife Conservation Commission (see table of layer sources) as our main data source. We also used a Florida Conservation Lands data layer from the Florida Natural Areas Inventory (see table layer of sources). After extracting the land cover and conservation data for the archaeological sites, we analyzed and classified each site into one of five land use categories: protected public land; private or wildland; developed open space; agriculture, low intensity development; medium or high intensity development (Reeder-Myers 2015, 439). A ranking of 1 was assigned to cells that were protected public land while a 5 was assigned to cells that had medium to high intensity development (Reeder-Myers 2015, 439).

We also explored the effect of hurricanes on shoreline erosion and accretion rates. NOAA's National Hurricane Center provides storm track files that contain storms ranging in strength from tropical depressions to category 5 hurricanes (NOAA, National Centers for Environmental Information). This dataset contains the dates of the storms, as well as their strength by wind speed. We removed tropical depressions from the dataset, and then extracted only hurricanes that cross the Florida Coast.

It must be noted that attempts to predict future vulnerability of areas to hurricane-related damages requires understanding complex natural and anthropogenic factors in spatial and temporal contexts, which would require a separate, multi-disciplinary hazard assessment project (Taramelli et al. 2008, 839-840). Understanding the potential shortcomings of our approach, we think it is an appropriate first step to quantifying hurricane impact on coastline by measuring storm frequency and storm strength. Frequency was determined by how many hurricanes pass over each of the archaeological sites. The area the hurricanes affected was determined using the radius of maximum wind (Malmstadt et al. 2009, 116-117). The hurricanes were buffered using the radius of maximum wind at the time of landfall. We then tallied up how many polygons that each site was in (Xu et al 2008, 1-2). The scores after being tallied will be interpolated and then normalized on a scale of 1 to 5, 1 representing the areas with the lowest amount of hurricane passes.

We used the wind speed at time of landfall to measure storm strength. The coastal area affected by RMW received the same strength score, with the area outside receiving a zero (Lin et al. 2014). Each site's total score will be divided by the total number of storms to strike the same site to produce the average hurricane strength.

Results and Discussion

We produced two separate rankings of vulnerability for Florida's coastal archaeological sites (Tables 1 and 2; Maps 1 and 2). The distance, elevation and land use classifications were the same for each set of rankings (Table 3). The difference between the two site vulnerability rankings comes from our use of different classification breaks for our shoreline vulnerability indices (Table 4). Our national classification system was the one used by the USGS coastal vulnerability study for the Gulf and Atlantic coasts (Thieler and Hammar-Klose 2000; Thieler and Hammar-Klose 1999). After classifying the raw data we collected for Florida for each coastal variable, the resulting histograms were non-normal, with a few variables showing Florida's coastline is more vulnerable than the national averages (Figure 3). We also created a classification system for Florida using Jenks natural breaks (Table 4), which placed the classification divisions where the largest distance between clusters existed (de Smith et al. 2015, "Classification and Clustering"). This created more normal distributions for our classified data (Figures 3-8).

Calculating CRVI (Figure 2) using each of these separate CVI classification systems did not produce any major differences (Tables 1 and 2; Maps 1 and 2). 13 site's vulnerability changed, but none by more than one (Map 3). When moving from the Florida classification to the National classification, seven sites moved from a vulnerability of high to moderate. Two sites moved from moderate to low, and two more from high to very high vulnerability. One site each moved from low to moderate and moderate to high vulnerability (Maps and 2). The Florida classification produced nine sites with a very high vulnerability (Table 2; Map 2), while the national classification included the same nine sites, with an additional two, in its most vulnerable category (Table 2; Map 2).

There was no clear geographic distribution of site vulnerability rankings (Maps 1 and 2). We then investigated whether there was any geographic correlation between the overall vulnerability classification and any individual variable's vulnerability classification. To do this,

we used the raster calculator to difference the classified values of the site vulnerability and each individual variable's vulnerability. This produced no conclusive pattern for any variable, with the differences being randomly scattered throughout the state.

We also calculated a Pearson's correlation matrix between the raw value of the coastal vulnerability and the classified values for each coastal variable (Table 5). We chose to use raw values for the coastal vulnerability and classified values for the variables because the classified values of variables were used to calculate a raw score for coastal vulnerability (Figure 2). The correlation matrix showed each coastal variable except for geomorphology had a significant correlation with CVI when using a 0.05 p-value. Historic erosion rate had a strong correlation with an *r*-value of 0.77 with a p-value less than 0.0001. Sea level rise had a moderate to strong correlation with and *r*-value of 0.57, while mean tidal range had a moderate correlation at 0.39. Coastal slope and mean wave height had weak correlations with CVI, with *r*-values of 0.27 and 0.24, respectively. These correlation results do not support Reeder-Myers' weighted formula for calculating shoreline vulnerability:

$$\mathrm{SV} = \frac{4(\mathrm{geomorph.} + \mathrm{CS} + \mathrm{SLR}) + 3(\mathrm{Eros.}) + 2(\mathrm{MWH} + \mathrm{TR})}{6}$$

The correlation coefficients suggest that erosion is the most important factor when calculating SV. Sea level rise and tidal range are moderately important, with coastal slope, mean wave height, and geomorphology having the lowest impact.

In addition, there were moderate correlations between erosion and SLR(r = 0.35), as well as erosion and MTR (r = 0.35). This could suggest that our formula for shoreline vulnerability has not captured all of the important factors for shoreline erosion rates. This, coupled with the significant correlation between erosion and site vulnerability, makes it important for future studies to examine if events, such as hurricanes, have any impact in explaining this correlation. We did not calculate a correlation matrix for CRVI values and variables because we used a weighted formula to produce CRVI values (Figure 2). Since we relied on precedent, rather than statistical evidence, when using the weights in the formula, any correlation results could not be justified in this paper.

Sources of Error and Uncertainty

The design of our study and definition of our key concepts (Figure 1) included some error and uncertainty. We were calculating vulnerability at sites that did not lay on the coast, so we had to use the closest point on the coast as representative of the coastal conditions for our sites. Since sites could be up to 5km from the coast, the accuracy of the shoreline vulnerability varies. Since this method has been used by other studies (Reeder-Myers 2015; Van Rensselaer 2014; Reeder et al. 2012; Westley et al. 2011), we felt this error was acceptable.

In addition, the results of our study are dependent on the accuracy of the data we used for each variable. Distance and elevation were relatively error free. The locations of the site polygons were provided by the Florida state archaeologist's office, and the DEM we used for elevation (see table of data sources) was the most accurate state-wide DEM derived from LiDAR data. The coastline we used to measure distance from sites to coast was recorded at a 1:150,001 – 1:600,000 scale (NOAA Office of Coastal Survey). This was the highest spatial resolution coastline we could find. Coastal LiDAR does not exist for the entire state of Florida, but a combination of the available coastal LiDAR and aerial imagery could allow for the creation of a more accurate current coastline. Unfortunately, time and resources did allow for the creation of such a coastline layer in this project.

Several of our variables have values recorded at only a handful of point locations, which we used to interpolate along the entire coast. This likely introduced some error into our project. Mean wave height was measured at 15 near-shore NOAA buoys (Map 4), sea level rise data was available at 15 NOS tidal stations (Map 5), and long-term erosion rates were calculated for certain stretches of the coast (Map 6). The USGS study used 28 tidal stations to interpolate tidal range along the entire Atlantic Coast (Thieler and Hammar-Klose 1999) and seven NOS data stations to interpolate sea level rise values along the Gulf coast (Thieler and Hammar-Klose 2000). Reeder-Myers drew from these datasets for her studies (Reeder-Myers 2015, 440; Reeder et al. 2012, 193) as well. Until researchers produce more accurate methods for recording coastal variables, error will be introduced by using relatively small numbers of raw data points and interpolating values along the coast in coastal vulnerability studies.

We are unable to verify the accuracy of our geomorphology data as well. The geomorphology variable measures the relative erodibility of the coastal landforms. No statewide dataset measuring the erodibility of coastal landforms exists for Florida. The state-wide land

cover dataset produced by the Florida Fish and Wildlife Conservation Commission did include some information on coastal landform type, but time and resources did not allow for an investigation of the erodibility of each landform type. Ultimately, we extracted the geomorphology classified scores from the USGS CVI studies (Thieler and Hammar-Klose 2000; Thieler and Hammar-Klose 1999) for each of our points along the coast representing the archaeological sites. Since the USGS dataset only included the geomorphology vulnerability ranking and not the original landform type, we were unable to create a separate Florida-based classification for geomorphology and all sites received a vulnerability score of 3, 4 or 5 in both classification systems (Figure 3).

Some error was likely introduced by the formulas we used to calculate shoreline vulnerability and site vulnerability (Figure 2). The formula for shoreline vulnerability used unweighted variables:

$$SV = \sqrt{\frac{a * b * c * d * e * f}{6}}$$

This assumes all physical variables have equal impact on the overall shoreline vulnerability, which we do not have evidence to support. Reeder-Myers did use a weighted formula to calculate her shoreline vulnerability (Reeder-Myers 2015, 439):

$$SV = \frac{4(a + b + c) + 3(d) + 2(e + f)}{6}$$

However, she did not explain the justification of the weighting. Ultimately, we used the unweighted formula because we thought the assumption that all physical variables had equal effect on shoreline vulnerability introduced less error.

The CRVI we used was a weighted formula created by Reeder-Myers. Her justification (Reeder-Myers 2015, 438; Reeder et al. 2012, 194) for this was to place the most emphasis on the location of the site in landscape, thus multiplying the combined distance and elevation classifications by two. Shoreline vulnerability was the next most important variable, thus receiving a weight of three. Modern land use at the site was the least important variable for calculating the vulnerability of an archaeological site, so it received a weight of two. However, there was no statistical evidence provided in her articles for the weights. Therefore, we cannot quantify the error introduced by the weights, but must assume that some error was introduced since her study areas did not include Florida.

$$\mathrm{CRV} = \frac{2(\mathrm{D} + \mathrm{E}) + 3(\mathrm{SV}) + 2(\mathrm{LU})}{3}$$

Conclusion and Future Research

We learned the difficulties of attempting a state-wide study using high-definition data. LiDAR data was available for many areas of the state, which we attempted to initially use. Unfortunately, any processing of these datasets on a statewide scale took over 24 hours and was not viable for this project. After producing a statewide vulnerability index, future research should be focused on regional studies and the development of more accurate formulas for calculating both site and coastal vulnerability. For example, focusing on the regions that had multiple very high vulnerability sites (Maps 1 and 2) would be good places to conduct regional studies. With a smaller study area, higher resolution topographic and bathymetric data could be used. Several coastal LiDAR datasets are available in certain areas of Florida between 1999 and 2014. Shorelines could be derived from each successive dataset to produce more accurate recent measures of shoreline change and erosion. With funding, researchers could analyze recent aerial photography and satellite imagery, or conduct field-studies, to record geomorphology. With higher quality data, researchers could produce weighted formulas that properly represent the impact of variables relative to each other for certain areas, which could then be reused in areas with similar coastal environments. It could also help researchers understand more fully the interactions between the variables.

Hurricane tracks were collected and generated by the National Oceanic and Atmospheric Administration's National Hurricane Center. Each track contains the storm name, number, wind speed, atmospheric pressure, radius of maximum wind, and the time that the reading was taken. The shapefile contained global hurricane tracks spanning back to 1842. The first thing that we did was select storms that intersected the Florida coastline and creating a new shapefile with only the intersecting storms. The tracks are then buffered using each individual radius of maximum wind. The hurricane frequency will be calculated by tallying how many buffer polygons encircle each point.

Comparing the normalized hurricane layers to the normalized erosion layers appeared to show that hurricanes did not have an effect on erosion levels of the Florida coast. The CVI of each showed that there was no positive or negative correlation connecting hurricane frequency

and strength with erosion rates. The analysis of these two variables was not accurate due to not having enough time to run a proper analysis, including correlation with potential error. The correlations gained here were based on the comparison of the erosion CVI with the hurricane frequency CVI. These two were divided and that number was used as a comparison. The closer the number was to zero indicated that the closer the two CVIs were to each other, meaning that the farther the numbers were from 1, the highest and lowest being 5 and 0.2 respectively. If more time were available for the project, a better correlation would be calculated.

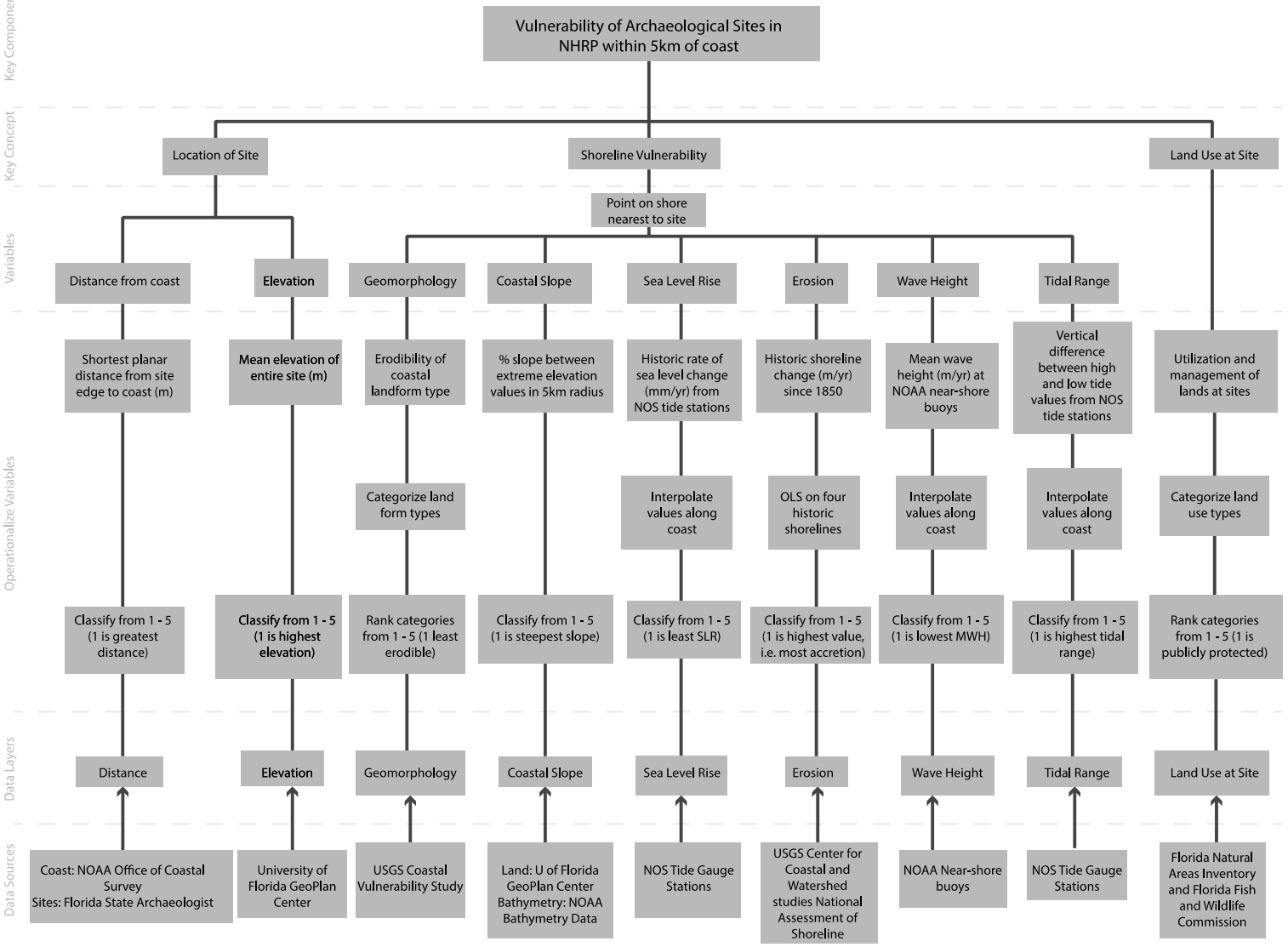

Figure 1: Conceptualization diagram

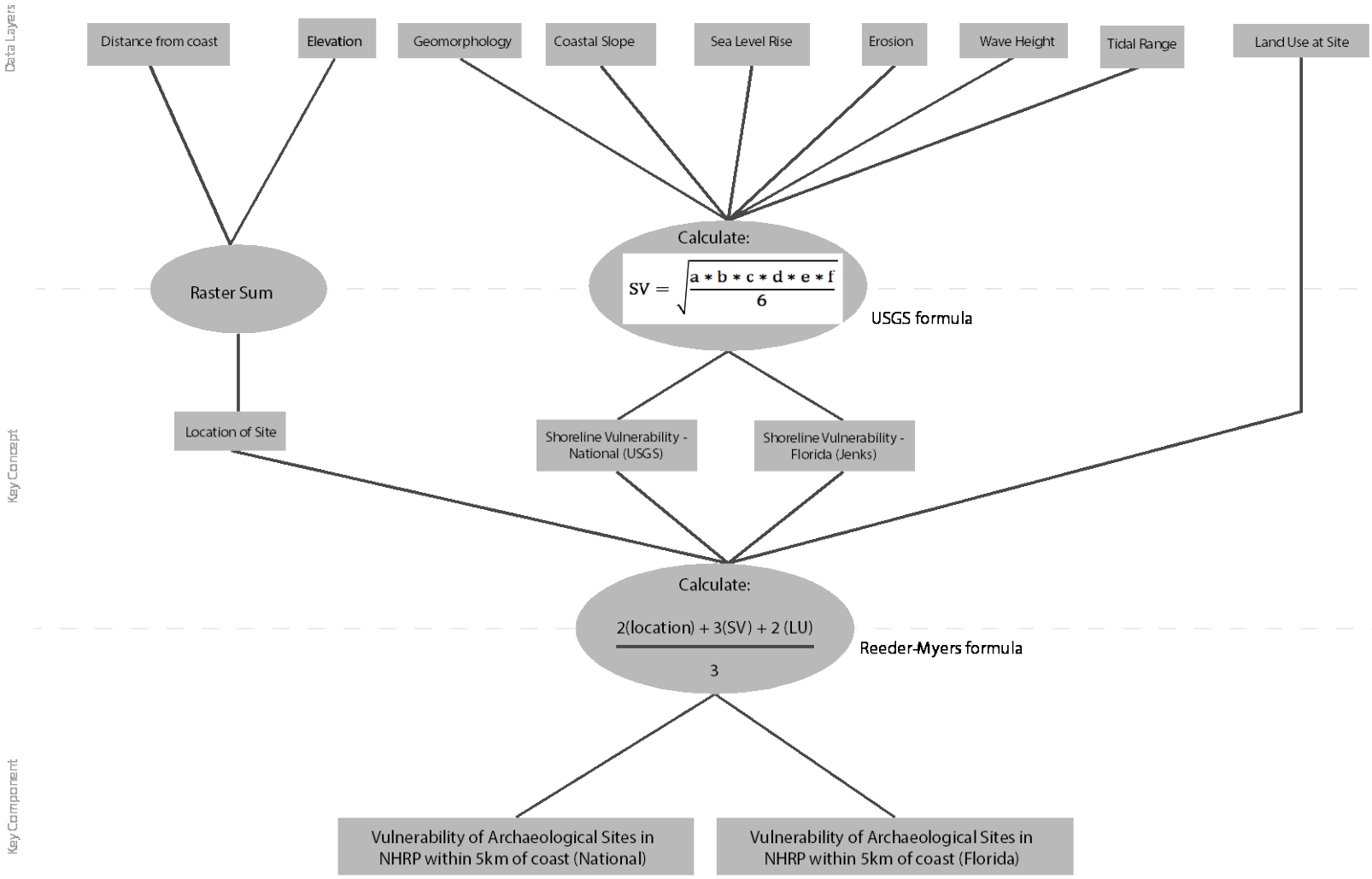

Figure 2: Implementation diagram

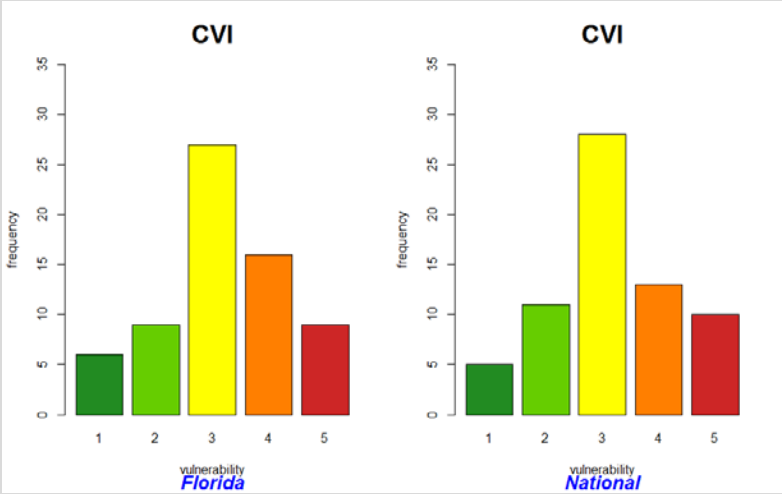

Figure 3: Histograms of classified CVI values using Florida and National classification systems (Table 4). The distributions were relatively similar, with categories 4 and 5 experiencing some relative changes.

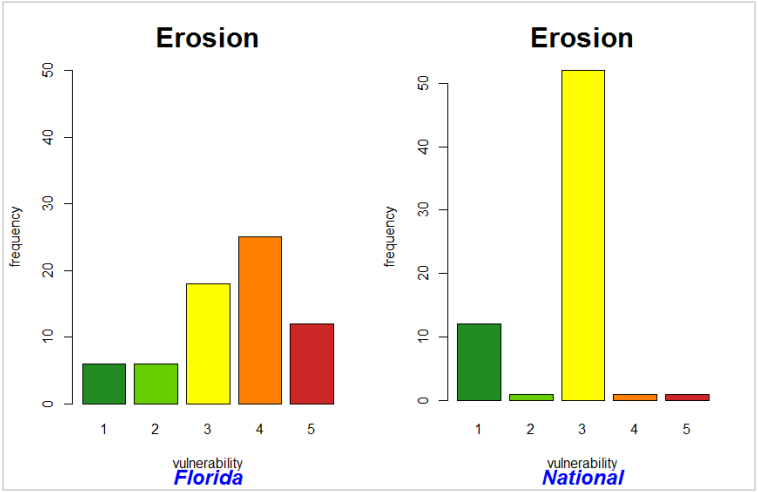

Figure 4: Histograms of classified erosion rate values using Florida and National classification systems (Table 4). A large majority of sites were classified as having moderate erosion in the national classification.

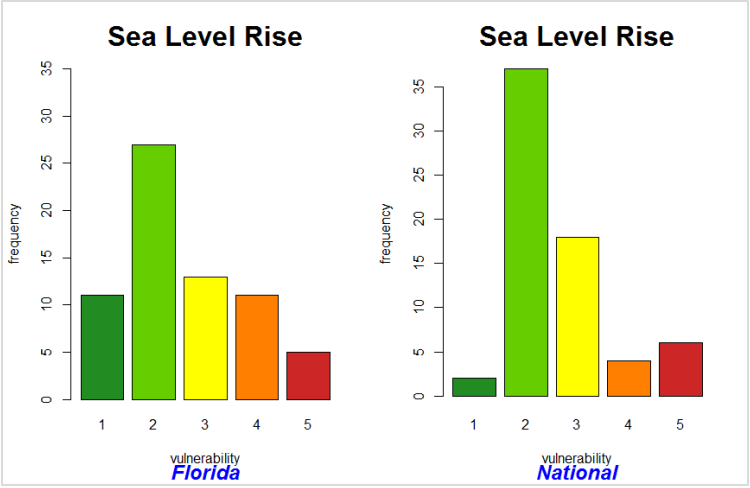

Figure 5: Histograms of classified sea level rise values using Florida and National classification systems (Table 4). The majority of our points had relatively low SLR values using the national system.

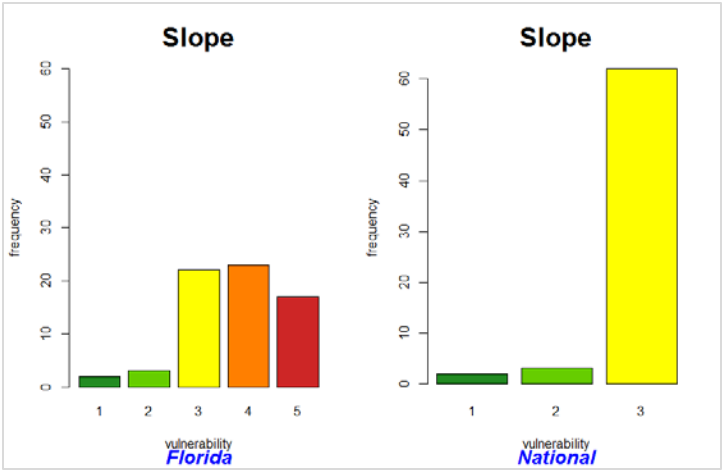

Figure 6: Histograms of classified coastal slope values using Florida and National classification systems (Table 4). Slope values in the National classification had much lower classifications.

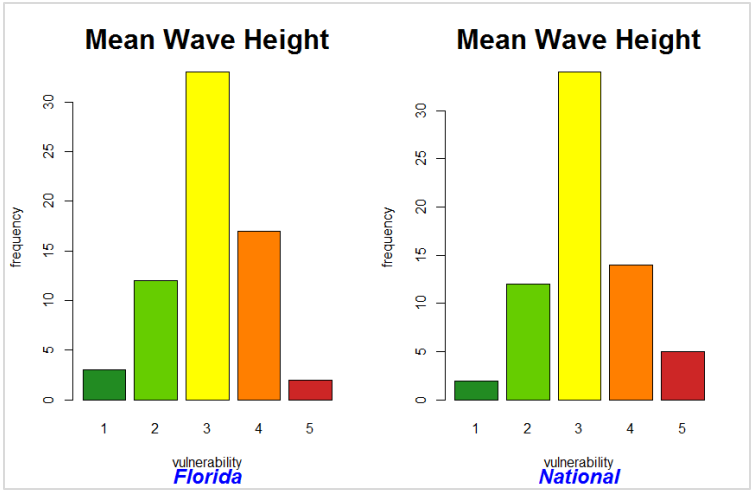

Figure 7: Histograms of classified mean wave height values using Florida and National classification systems (Table 4). The distributions were very similar, with a few scores moving from category 4 to 5 in the National system.

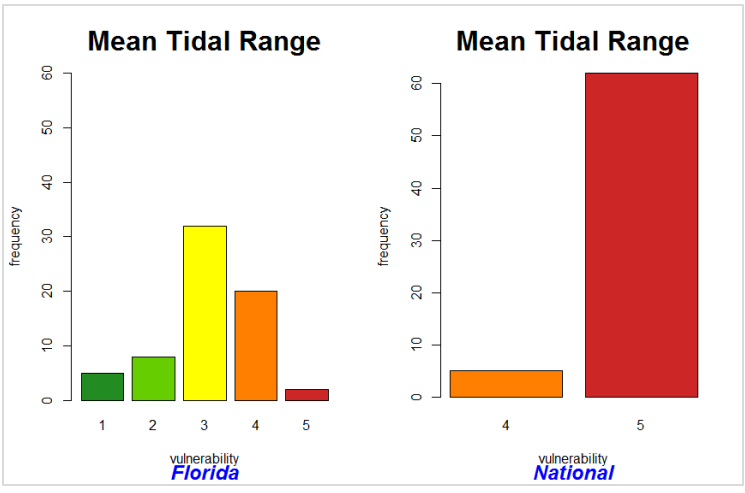

Figure 8: Histograms of classified mean tidal range values using Florida and National classification systems (Table 4). Our coastal points had very low tidal ranges, which led to all sites being classified as a 4 or 5 vulnerability in the national classification.

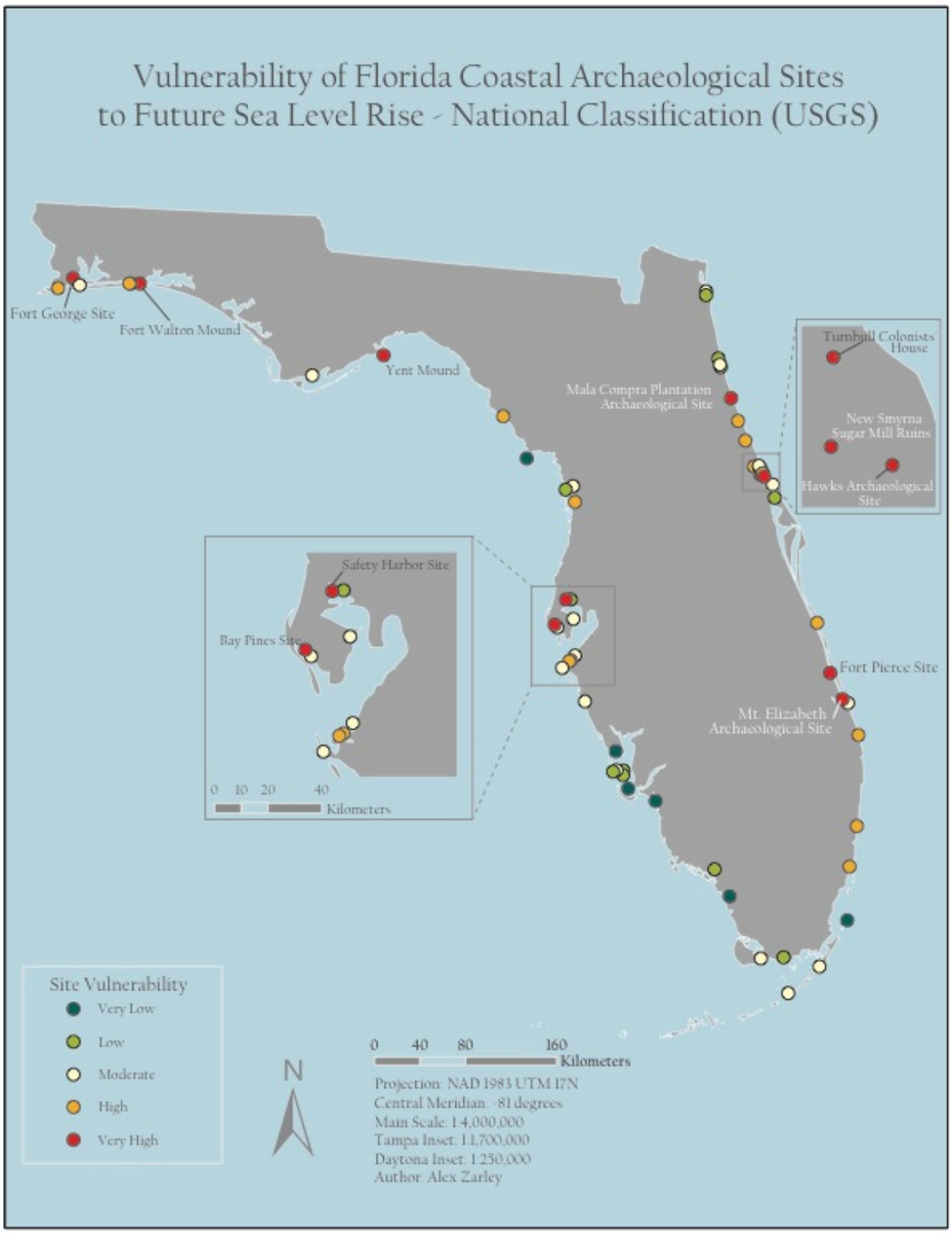

Map 1: Site vulnerability classifications calculated using the National CVI classifications (Table 4). All sites with a Very High vulnerability are labeled.

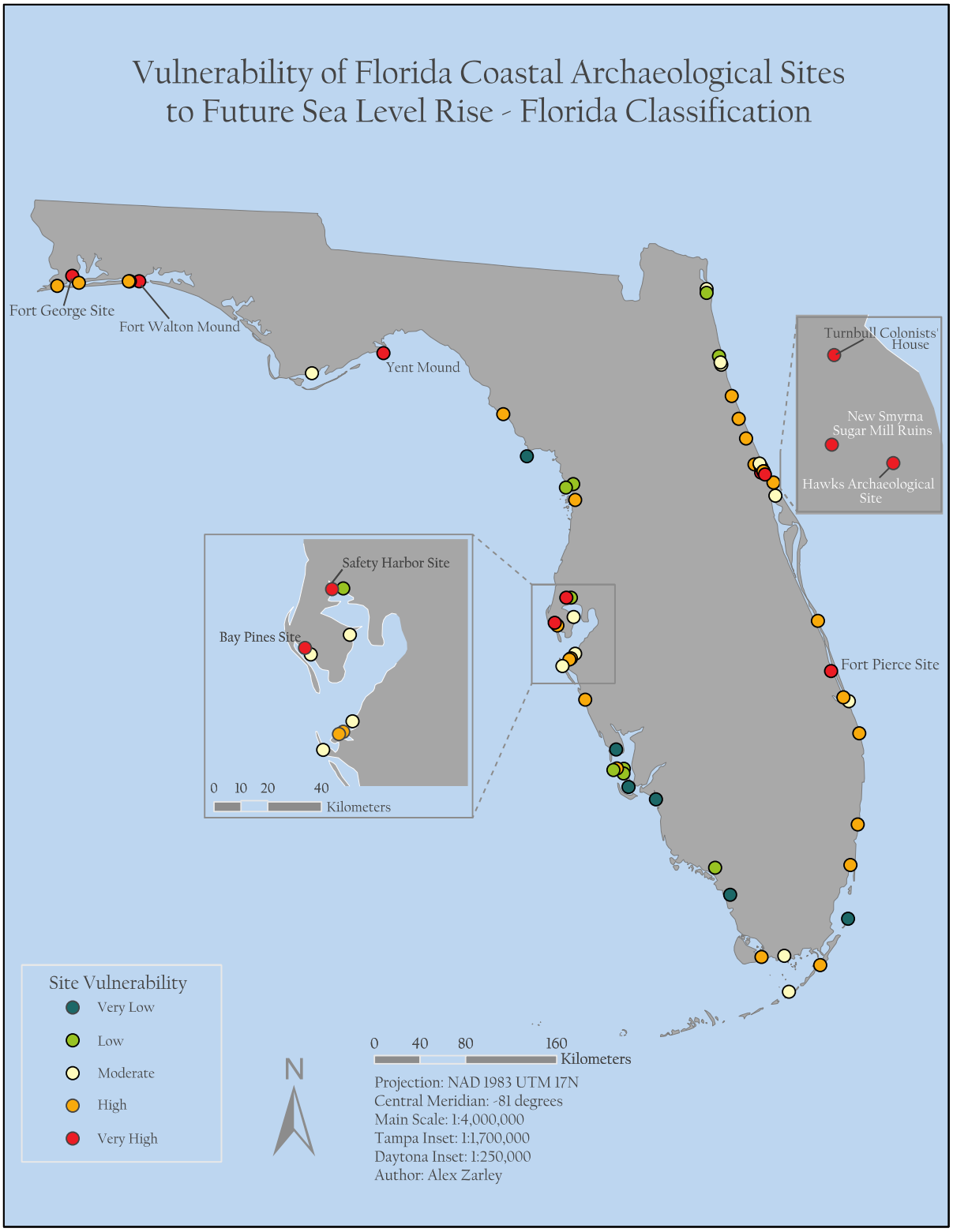

Map 2: Site vulnerability classifications calculated using the Florida CVI classifications (Table 4). All sites with a Very High vulnerability are labeled.

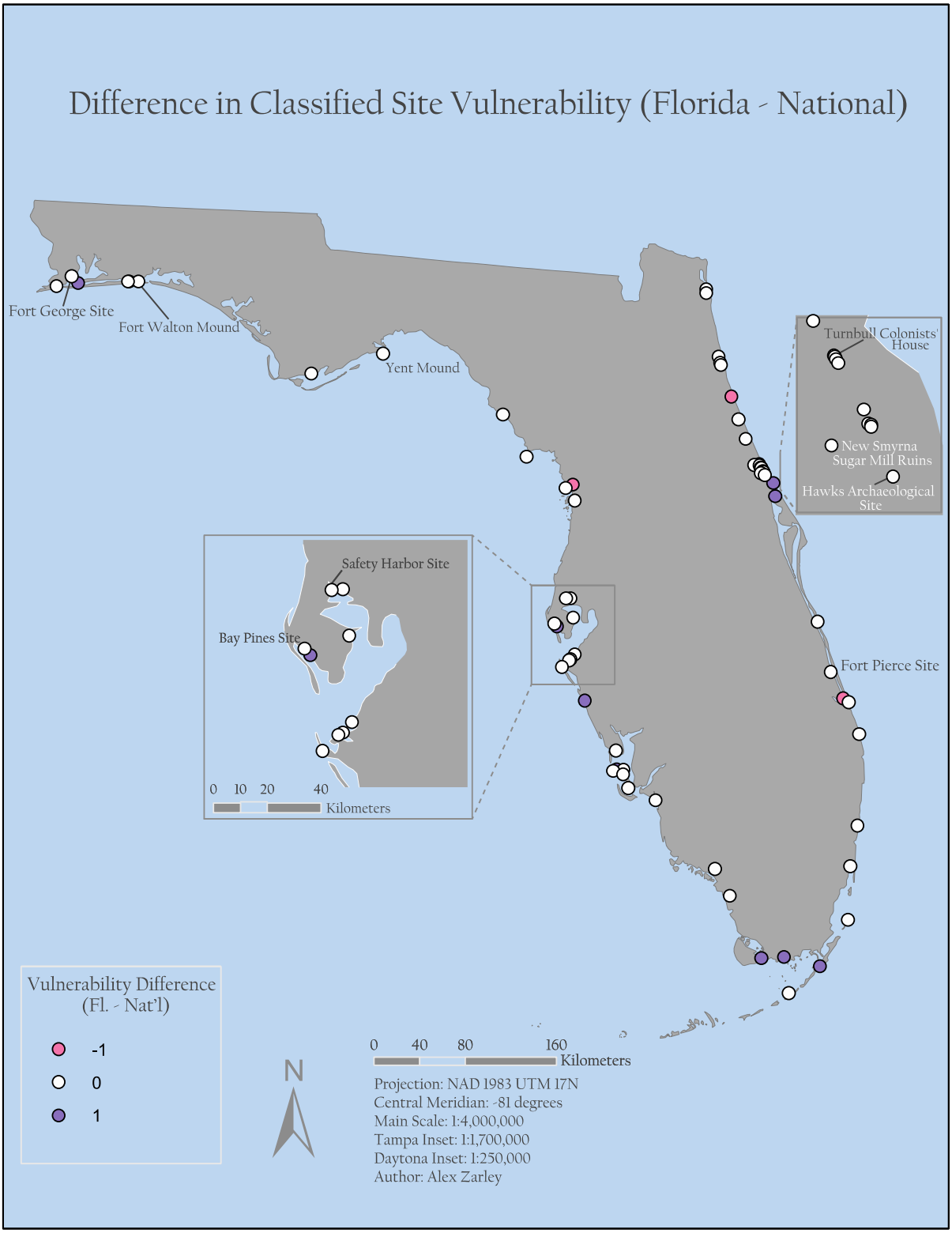

Map 3: Difference in site vulnerability values between the Florida and National classification systems. Differences were calculated by subtracting CRVI classified values produced by the National CVI classifications from the CRVI classified values produced using the Florida system.

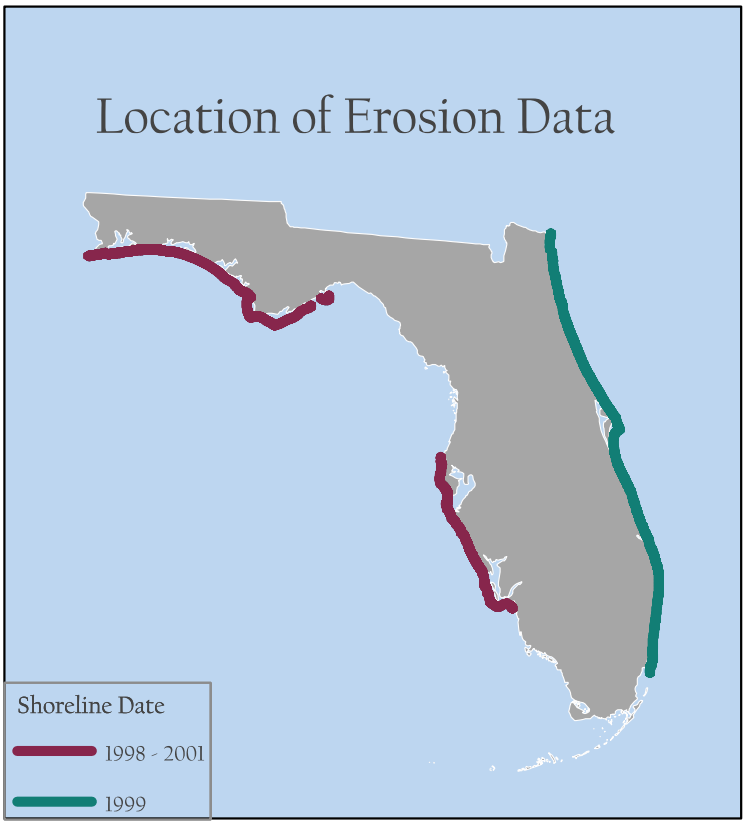

Map 6: Location of erosion rates data.

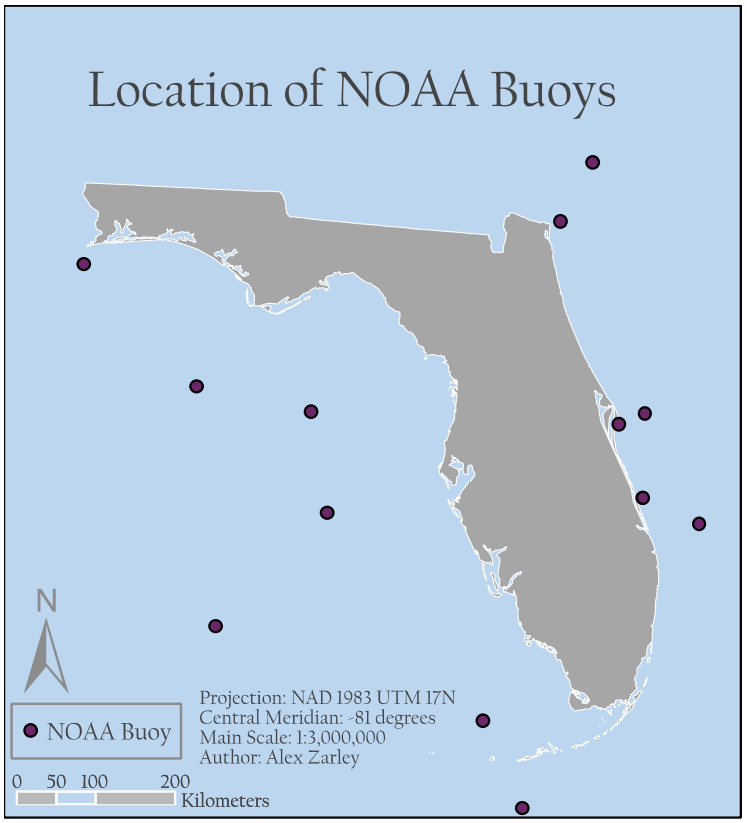

Map 4: Location of NOAA buoys with MWH data.

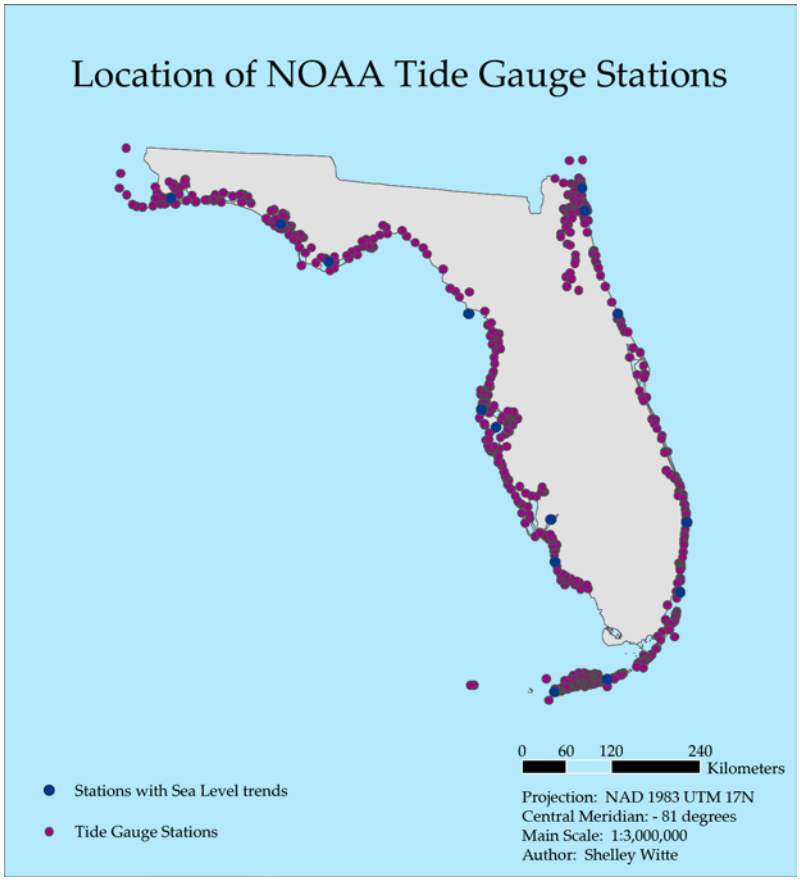

Map 5: Location of Tide Gauge Stations for Sea Level Rise and Tidal Range data

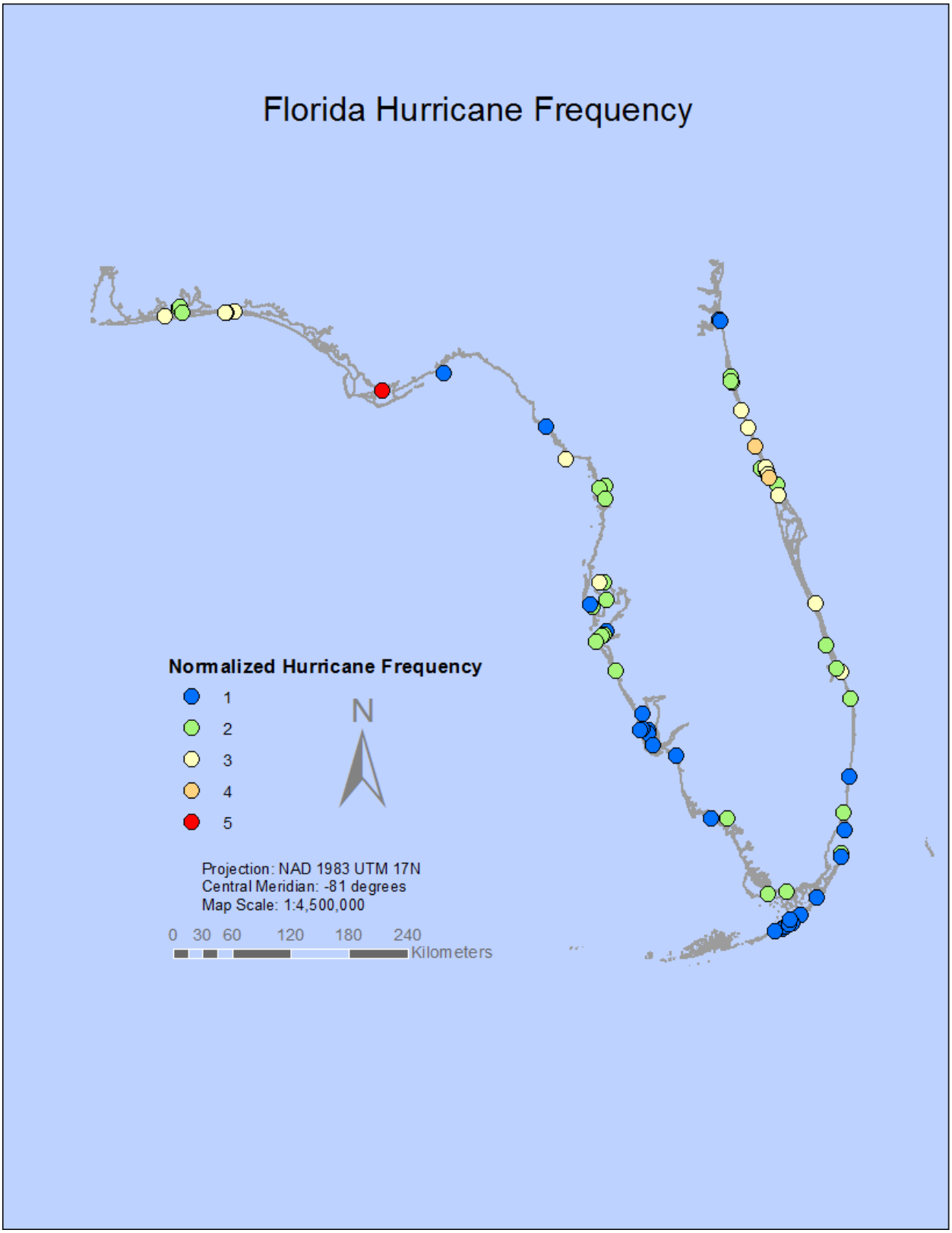

Map 7: Normalized Hurricane frequency at the coastal archaeological sites

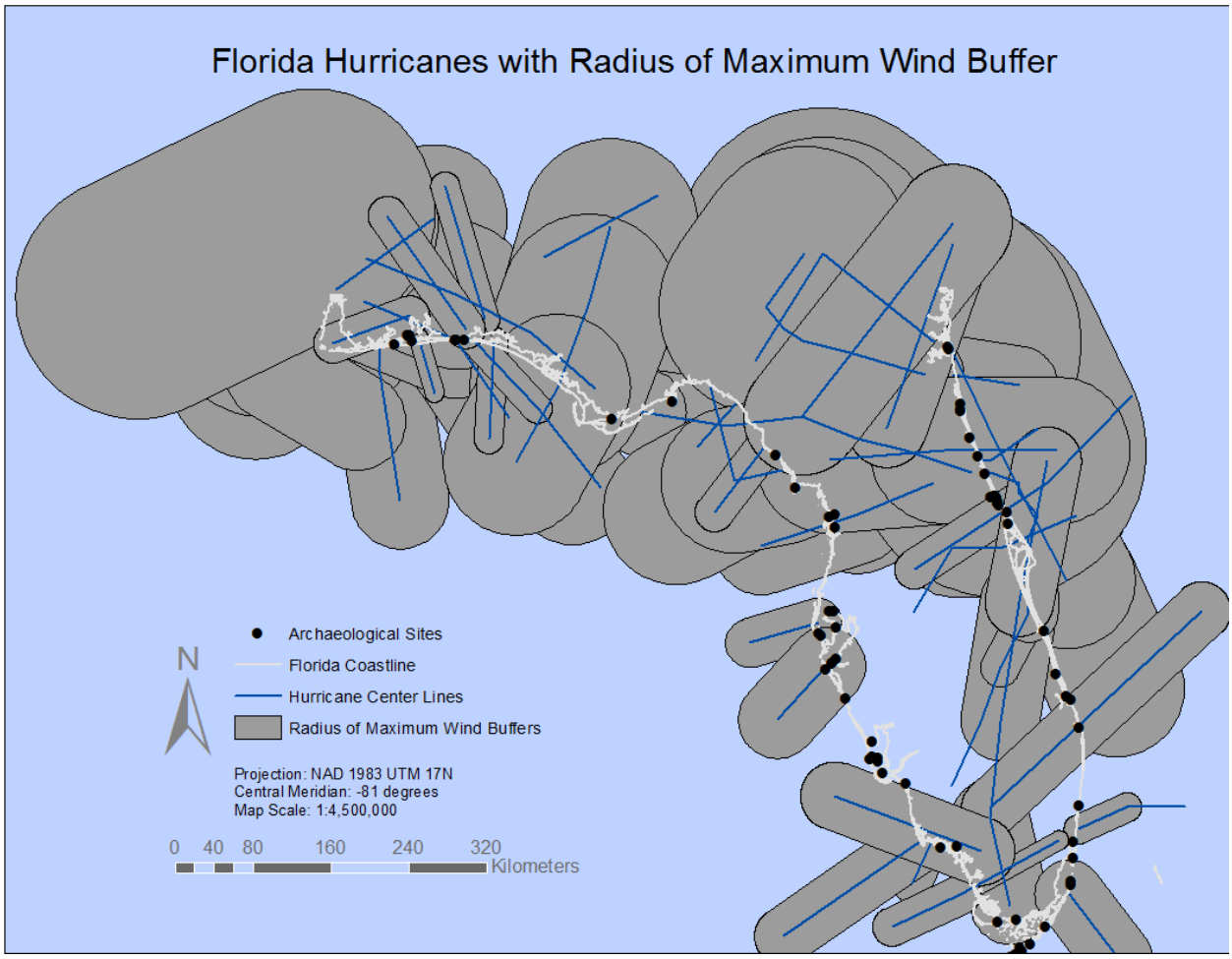

Map 8: Hurricanes crossing the Florida coast line with the storms buffered using the Radius of Maximum Wind (RMW). Coastal archaeological sites are represented as the black dots on the map.

National Classification (USGS)		
Rank	Site Name	CRVI Value
1	Fort George Site	5
2	Fort Walton Mound	5
3	Bay Pines Site (8Pi64)	5
3	New Smyrna Sugar Mill Ruins	5
3	Turnbull Colonists' House Archeological Site	5
6	Safety Harbor Site	5
6	Mala Compra Plantation Archeological Site	5
8	Yent Mound	5
8	Fort Pierce Site	5
8	Hawks Archeological Site	5
8	Mount Elizabeth Archeological Site	5
12	Airport Clear Zone Archeological Site	4
12	Janet's Archeological Site	4
14	World War II JB--2 Mobile Launch Site	4
15	Pompano Beach Mound	4
15	Arch Creek Historic and Archeological Site	4
15	Spruce Creek Mound Complex	4
15	Three Chimneys Archaeological Site	4
15	Grange Archeological Site	4
15	Turnbull Colonists' House No. 2 Archeological Site	4
15	First Presbyterian Church Archeological Site	4
15	Hickory Ridge Cemetery Archeological Site	4
15	Spanish Fleet Survivors and Salvors Camp Site	4
24	Yulee Sugar Mill Ruins	4
24	Jupiter Inlet Historic and Archeological Site	4
24	World War II JB--2 Launch Site	4
27	Garden Patch Archeological Site (8Di4)	4
27	Bulow Plantation Ruins	4
27	Portavant Mound Site	4
27	Shaw's Point Archeological District	4
27	Old Fort Park Archeological Site	4
27	Blanchette Archeological Site	4
33	Bear Lake Mounds Archeological District	3
33	Jungle Prada Site	3
33	Butcherpen Mound	3
33	Sanchez Powder House Site	3
37	Useppa Island Site	3
37	Rock Mound Archeological Site	3
37	Madira Bickel Mounds	3
37	Regina Shipwreck Site	3
37	Old Stone Wharf Archeological Site	3
42	Osprey Archeological and Historic Site	3
42	Pierce Site	3
42	Fish Island Site	3
42	Crystal River Indian Mounds	3
46	Turtle Mound	3
46	Grand Site	3
46	Georges Valentine Shipwreck Site	3
46	Sleepy Hollow Archeological Site	3
50	Lignumvitae Key Archeological and Historical District	3
50	Weeden Island Site	3
52	Mission of San Juan del Puerto Archeological Site	2
52	Fort Mose Site, Second	2
54	Monroe Lake Archeological District	2
54	Mullet Key	2
56	Ross Hammock Site	2
57	Pineland Archeological District	2
57	Josslyn Island Site	2
57	Upper Tampa Bay Archeological District	2
60	Halfway Creek Site	2
60	Pardo, Mark Shellworks Site	2
62	Big Mound Key--Boggess Ridge Archeological District	1
62	Sweeting Homestead	1
64	Cedar Keys Historic and Archaeological District	1
65	Mound Key Site	1
66	Galt Island Archeological District	1
67	Ten Thousand Islands Archeological District	1

Table 1: Ranking of Site vulnerability using the National Classification system for shoreline vulnerability (see Table 4).

Florida Classification (Jenks)		
Rank	Site Name	CRVI Value
1	Fort George Site	5
2	Yent Mound	5
3	Bay Pines Site (8Pi64)	5
3	New Smyrna Sugar Mill Ruins	5
3	Turnbull Colonists' House Archeological Site	5
6	Safety Harbor Site	5
7	Fort Pierce Site	5
7	Hawks Archeological Site	5
7	Fort Walton Mound	5
10	Airport Clear Zone Archeological Site	4
10	Janet's Archeological Site	4
10	Mala Compra Plantation Archeological Site	4
13	Mount Elizabeth Archeological Site	4
14	Bear Lake Mounds Archeological District	4
14	Pompano Beach Mound	4
14	Arch Creek Historic and Archeological Site	4
14	Spruce Creek Mound Complex	4
14	Three Chimneys Archaeological Site	4
14	Grange Archeological Site	4
14	Turnbull Colonists' House No. 2 Archeological Site	4
14	First Presbyterian Church Archeological Site	4
22	Useppa Island Site	4
22	Rock Mound Archeological Site	4
22	Yulee Sugar Mill Ruins	4
22	Jupiter Inlet Historic and Archeological Site	4
26	Osprey Archeological and Historic Site	4
26	Garden Patch Archeological Site (8Di4)	4
26	Bulow Plantation Ruins	4
26	Portavant Mound Site	4
26	Shaw's Point Archeological District	4
26	Old Fort Park Archeological Site	4
26	Blanchette Archeological Site	4
26	World War II JB--2 Mobile Launch Site	4
34	Turtle Mound	4
34	Jungle Prada Site	4
34	Butcherpen Mound	4
34	Hickory Ridge Cemetery Archeological Site	4
34	Spanish Fleet Survivors and Salvors Camp Site	4
39	Madira Bickel Mounds	3
39	Regina Shipwreck Site	3
39	Old Stone Wharf Archeological Site	3
39	World War II JB--2 Launch Site	3
43	Pierce Site	3
43	Fish Island Site	3
45	Monroe Lake Archeological District	3
45	Grand Site	3
45	Georges Valentine Shipwreck Site	3
45	Sleepy Hollow Archeological Site	3
45	Sanchez Powder House Site	3
50	Ross Hammock Site	3
50	Lignumvitae Key Archeological and Historical District	3
50	Weeden Island Site	3
53	Pineland Archeological District	2
53	Josslyn Island Site	2
53	Mission of San Juan del Puerto Archeological Site	2
53	Crystal River Indian Mounds	2
57	Halfway Creek Site	2
57	Pardo, Mark Shellworks Site	2
59	Upper Tampa Bay Archeological District	2
59	Fort Mose Site, Second	2
61	Mullet Key	2
62	Big Mound Key--Boggess Ridge Archeological District	1
62	Sweeting Homestead	1
64	Galt Island Archeological District	1
65	Ten Thousand Islands Archeological District	1
65	Mound Key Site	1
67	Cedar Keys Historic and Archaeological District	1

Table 2: Ranking of Site vulnerability using the Florida Classification system for shoreline vulnerability (see Table 4).

	Site Vulnerability Classifications				
Variable	Very Low 1	Low 2	Moderate 3	High 4	Very High 5
Elevation (m)	>5.62	5.62 - 2.27	2.27 - 1.28	1.28 - 0.98	<0.98
Distance (m)	>1006.16	1006.16 - 246.70	246.70 - 58.32	58.32 - 11.59	<11.59
CVI (Raw)	<5.10	5.10 - 9.80	9.80 - 14.14	14.14 - 21.91	> 21.91
Land Use	Protected public land	Private, wildland	Developed open space, agriculture	Developed, low intensity	Developed, medium to high intensity
CRVI (Raw)	<5.00	5.0 - 7.32	7.32 - 8.66	8.66 - 10.35	> 10.35

Table 3: Vulnerability categories and the breakpoints used to calculate site vulnerability. Distance and elevation were classified using arithmetic intervals. CVI and CRVI raw values were classified using Jenks natural breaks. Land use is a categorical variable.

		Coastal Vulnerability Classifications				
Variable	Vulnerability	Very Low 1	Low 2	Moderate 3	High 4	Very High 5
Geomorphology	National	Rocky, cliffed coasts; Fjords	Medium cliffs; indented coasts	Low cliffs; glacial drift; alluvial plains	Cobble beaches; estuary; lagoon	Barrier beaches; sand beaches; salt marsh; mud flats; deltas
	Florida					
Coastal Slope (%)	National	> 0.2	0.2 - 0.07	0.07 - 0.04	0.04 - 0.025	< 0.25
	Florida	> 1.75	1.75 - 0.99	0.99 - 0.49	0.49 - 0.27	< 0.27
Relative sea-level change (mm/yr)	National	< 1.8	1.8 - 2.5	2.5 - 2.95	2.95 - 3.16	> 3.16
	Florida	< 2.04	2.04 - 2.39	2.39 - 2.79	2.79 - 3.18	> 3.18
Shoreline erosion/accretion (m/yr)	National	> 2.0	2.0 - 1.0	1.0 - -1.0	-1.1 - -2	< -2.0
	Florida	> 3.29	3.29 - 1.47	1.47 - 0.25	0.25 - -0.44	< -0.44
Mean Tide Range (m)	National	> 6.0	6.0 - 4.1	4.1 - 2.0	2.0 - 1.0	< 1.0
	Florida	> 0.88	0.88 - 0.65	0.65 - 0.40	0.40 - -0.95	< -0.95
Mean Wave Height (m)	National	< 0.55	0.55 - 0.85	0.85 - 1.05	1.05 -1.25	> 1.25
	Florida	< 0.66	0.65 - 0.86	0.86 1.03	1.03 - 1.30	> 1.30

Table 4: Vulnerability categories and the breakpoints used to calculate coastal vulnerability for each variable in each of our classification systems. National classification refers to the values used in the USGS CVI study.

Pearson's Correlation Coefficient Matrix							
	Geomorph	CS	SLR	MWH	MTR	Erosion	CVI_Raw
Geomorph	1	-0.01	0.09	0.04	0.15	-0.05	0.23
CS	-0.01	1	0.01	-0.22	-0.06	0.1	0.27
SLR	0.09	0.01	1	-0.27	-0.11	0.35	0.57
MWH	0.04	-0.22	-0.27	1	0.03	0.16	0.24
MTR	0.15	-0.06	-0.11	0.03	1	0.35	0.39
Erosion	-0.05	0.1	0.35	0.16	0.35	1	0.77
CVI_Raw	0.23	0.27	0.57	0.24	0.39	0.77	1

P Values							
	Geomorph	CS	SLR	MWH	MTR	Erosion	CVI_Raw
Geomorph	--	0.9104	0.4465	0.7313	0.2228	0.7172	0.0602
CS	0.9104	--	0.925	0.0768	0.6407	0.4029	0.0271
SLR	0.4465	0.925	--	0.0289	0.3938	0.0041	0.00
MWH	0.7313	0.0768	0.0289	--	0.7893	0.1924	0.0529
MTR	0.2228	0.6407	0.3938	0.7893	--	0.0042	0.0012
Erosion	0.7172	0.4029	0.0041	0.1924	0.0042	--	0.00
CVI_Raw	0.0602	0.0271	0.00	0.0529	0.0012	0.00	--

Table 5: Pearson's correlation coefficient matrix and p values. Coefficients were calculated using the raw CVI scores and the classified values for the other variables. Highlighted variables have less than a 5% chance of being associated solely as a result of chance. The correlation of CVI and MWH had a 5.29% chance of being solely due to chance, so it is highlighted in a slightly lighter color.

Table of Data Layer Sources

Layer	definition	GIS data source(s)	Website
geomorphology	erodibility of landform types	USGS CVI	https://pubs.usgs.gov/dds/dds68/htmldocs/data.htm
coastal slope	Percent change between highest/lowest elevations within 5km radius of coastal cells	University of Florida GeoPlan Center (land) / NOAA NGDC Coastal DEMs (bathymetry)	https://www.gisinventory.net/GISI-24441-FLORIDA-DIGITAL-ELEVATION-MODEL-DEM-MOSAIC-5-METER-CELL-SIZE-ELEVATION-UNITS-CENTIMETERS-Digital-Elevation-Model.html https://www.ngdc.noaa.gov/dem/squareCellGrid/map
relative SLR	historic rates of change in mean water height)	NOS Tide Gauge Stations	http://tidesandcurrents.noaa.gov/stations.html?type=Water+Levels
historical erosion	shoreline change from 1850 until 1999	USGS Center for Coastal and Watershed Studies	http://coastal.er.usgs.gov/shoreline-change/
wave height	measured distance between wave trough to wave crest	NOAA buoys - Standard Meteorological	http://www.ndbc.noaa.gov/
land use	utilization and management of land	FL Fish and Wildlife Conservation Commission	http://myfwc.com/research/gis/applications/articles/Cooperative-Land-Cover
Site Distance	Shortest distance from site to coast	NOAA ENC	http://encdirect.noaa.gov/
Site elevation	mean elevation of site	University of Florida GeoPlan Center	https://www.gisinventory.net/GISI-24441-FLORIDA-DIGITAL-ELEVATION-MODEL-DEM-MOSAIC-5-METER-CELL-SIZE-ELEVATION-UNITS-CENTIMETERS-Digital-Elevation-Model.html
tidal range	mean vertical distance between highest and lowest tide elevations	NOS Tide Gauge Stations	original layer - http://tidesandcurrents.noaa.gov/stations.html?type=Water+Levels
hurricanes	storm strength and frequency	NOAA Hurricane Center	http://www.nhc.noaa.gov/

Bibliography

De Smith, Michael J., Michael F. Goodchild and Paul A. Longley. *Geospatial Analysis, 5th ed.* Accessed April 30, 2016. http://www.spatialanalysisonline.com/HTML/index.html.

Digital Coast. "Coastal Lidar Datasets at NOAA". Accessed March 5, 2016. https://coast.noaa.gov/htdata/lidar1_z/index.html

Erlandson, Jon M. "Racing a Rising Tide: Global Warming, Rising Seas, and the Erosion of Human History." *The Journal of Island and Coastal Archaeology* 3, no. 2 (2008): 167-169.

ESRI. "How Spline Works." Accessed May 6, 2016. http://pro.arcgis.com/en/pro-app/tool-reference/3d-analyst/how-spline-works.htm.

ESRI. "Spline." Accessed May 6, 2016. http://desktop.arcgis.com/en/arcmap/10.3/tools/spatial-analyst-toolbox/spline.htm.

Fitzpatrick, Scott M., Michiel Kappers, and Quetta Kaye. "Coastal Erosion and Site Destruction on Carriacou, West Indies." *Journal of Field Archaeology* 31, no. 3 (2006): 251–62.

Fitzpatrick, Scott Michael. "On the Shoals of Giants: Natural Catastrophes and the Overall Destruction of the Caribbean's Archaeological Record." *Journal of Coastal Conservation* 16, no. 2 (July 10, 2010): 173–86.

Florida Oceans and Coastal Council. 2010. "Climate Change and Sea-Level Rise in Florida: An Update of 'The Effects of Climate Change on Florida's Ocean and Coastal Resources.' [2009 Report]". Tallahassee, Florida.

Gornitz, V.M., T.W. Beaty, and R.C. Daniels,. "A Coastal Hazards Data Base for the U.S. West Coast." U.S. Department of Energy. December 1997.

IPCC, 2014: *Climate Change 2014: Synthesis Report. Contribution of Working Groups I, II and III to the Fifth Assessment Report of the Intergovernmental Panel on Climate Change* [Core Writing Team, R. K. Pachauri and L.A. Meyer (eds.)]. IPCC, Geneva, Switzerland.

Lin, N., P. Lane, K. A. Emanuel, R. M. Sullivan, and J. P. Donnelly (2014), Heightened hurricane surge risk in northwest Florida revealed from climatological-hydrodynamic modeling and paleorecord reconstruction, J. Geophys. Res. Atmos., 119, 8606–8623.

Malmstadt, Jill, Kelsey Scheitlin, James Elsner. "Florida Hurricanes and Damage Costs." *Southeastern Geographer* 49, no. 2 (2009): 108-131.

Morton, Robert A., Tara L. Miller, Laura J. Moore. 2004. *National Assessment of Shoreline Change: Part 1 Historical Shoreline Changes and Associated Coastal Land Loss Along the U.S. Gulf of Mexico*. U.S. Geological Survey Open-file Report 2004-1043.

Morton, Robert A., Tara L. Miller. 2005. *National Assessment of Shoreline Change: Part 2 Historical Shoreline Changes and Associated Coastal Land Loss Along the U.S. Southeast Atlantic Coast*. U.S. Geological Survery Open-file Report 2005-1401.

National Coastal Ecosystems Team (US). *Florida Ecological Atlas*. Fish and Wildlife Service, Division of Biological Services, National Coastal Ecosystems Team and the Minerals Management System, 1983.

New Mexico's Indicator-Based Information System (NM-IBIS). "Data Grouping Options for NM-IBIS Maps." Accessed April 30, 2016. https://ibis.health.state.nm.us/resource/MapChoroClasses.html

NOAA, National Centers for Environmental Information. "IBTrACS - International Best Track Archive for Climate Stewardship." Accessed March 10, 2016. http://www.ncdc.noaa.gov/ibtracs/index.php?name=ibtracs-data.

NOAA Office of Coastal Survey, "Coastal Data." Accessed April 2, 2016. http://encdirect.noaa.gov/.

NOAA, Tides & Currents - Sea Level Trends. Accessed on May 6, 2016. http://tidesandcurrents.noaa.gov/sltrends/sltrends.html.

NOAA, Tides & Currents – GetObservation Operation. Accessed on May 6, 2016. http://opendap.co-ops.nos.noaa.gov/ioos-dif-sos/index.jsp.

Noss, Reed F. "Between the Devil and the Deep Blue Sea: Florida's Unenviable Position with Respect to Sea Level Rise." *Climatic Change* 107, no. 1–2 (July 2011): 1–16.

Reeder, Leslie A., Torben C. Rick, and Jon M. Erlandson. "Our Disappearing Past: A GIS Analysis of the Vulnerability of Coastal Archaeological Resources in California's Santa Barbara Channel Region." *Journal of Coastal Conservation* 16, no. 2 (2012): 187–97.

Reeder-Myers, Leslie A. "Cultural Heritage at Risk in the Twenty-First Century: A Vulnerability Assessment of Coastal Archaeological Sites in the United States." *The Journal of Island and Coastal Archaeology* 10, no. 3 (September 2, 2015): 436–45.

———. E-mail message to authors, March 1, 2016.

Revell, David L., Robert Battalio, Brian Spear, Peter Ruggiero, and Justin Vandever. “A Methodology for Predicting Future Coastal Hazards due to Sea-Level Rise on the California Coast.” *Climatic Change* 109, no. 1 (December 10, 2011): 251–76.

Robinson, Michael H., Clark R. Alexander, Chester W. Jackson, Christopher P. McCabe, and David Crass. “Threatened Archaeological, Historic, and Cultural Resources of the Georgia Coast: Identification, Prioritization and Management Using GIS Technology.” *Geoarchaeology* 25, no. 3 (May 1, 2010): 312–26.

Saha, Amartya K., Sonali Saha, Jimi Sadle, Jiang Jiang, Michael S. Ross, Rene M. Price, Leonel S. L. O. Sternberg, Kristie S. Wendelberger. “Sea level rise and South Florida coastal forests.” *Climatic Change* (2011) 107: 81–108.

Tarameli, A., L. Melelli, M. Pasqui, A. Sorichetta. “Estimating hurricane hazards using a GIS system.” *National Hazards Earth Systems Science* 8 (2008): 839 – 854.

Thieler, E. R. and E. S. Hammar-Klose. 1999. *National Assessment of Coastal Vulnerability to Sea-Level Rise: Preliminary Results for the U.S. Atlantic Coast*. U.S. Woods Hole, MA: Geological Survey Open-File Report 99-593.

Thieler, E. R. and E. S. Hammar-Klose. 2000. *National Assessment of Coastal Vulnerability to Sea-Level Rise: Preliminary Results for the U.S. Gulf of Mexico Coast*. U.S. Woods Hole, MA: Geological Survey Open-File Report 00-179.

Van Rensselaer, Maximillian. “A GIS Analysis of Environmental and Anthropogenic Threats to Coastal Archaeological Sites in Southern Monterey County, California.” *SCA Proceedings* vol. 28 (2014): 273–80.

Wanless, Haorld R., Randall W. Parkinson and Lenore P. Tedesco, “Sea Level Control on Stability of Everglades Wetlands.” In: Davis SM, Davis Ogden JC (eds) *Everglades: the ecosystem and its restoration*. St. Lucie, Boca Raton (1994), pp 198–224.

Westley, Kieran, Trevor Bell, M. A. P. Renouf, and Lev Tarasov. “Impact Assessment of Current and Future Sea-Level Change on Coastal Archaeological Resources—Illustrated Examples From Northern Newfoundland.” *Journal of Island and Coastal Archaeology* 6, no. 3 (2011): 351-374.

Le Xu and R. E. Brown, "Hurricane simulation for Florida utility damage assessment," 2008 IEEE/PES *Transmission and Distribution Conference and Exposition*, Chicago, IL, 2008, pp. 1-6.